Embedding Human Expert Cognition into Autonomous UAS Trajectory Planning

Pritesh Narayan, Patrick Meyer and Duncan Campbell, *Member, IEEE*

***Abstract*—This paper presents a new approach for the inclusion of human expert cognition into autonomous trajectory planning, for Unmanned Aerial Systems (UAS) operating in low altitude environments. During typical UAS operations, multiple objectives may exist, therefore the use of Multi-Criteria Decision Aid (MCDA) techniques can potentially allow for convergence to trajectory solutions which better reflect overall mission requirements. In that context, additive Multi-Attribute Value Theory (MAVT) has been applied to optimize trajectories with respect to multiple objectives. A Graphical User Interface (GUI) was developed to allow for knowledge capture from a Human Decision Maker (HDM) through simulated decision scenarios. The expert decision data gathered, is converted into value functions and corresponding criteria weightings using UTility Additive (UTA) theory. The inclusion of preferences elicited from HDM data within an Automated Decision System (ADS) allows for the generation of trajectories which more closely represent the candidate HDM's decision preferences. This approach has been demonstrated in this paper through simulation using a fixed wing UAS operating in low altitude environments.**

***Index Terms*—Unmanned Aircraft, Unmanned Aerial System, Trajectory, Autonomous, Multi-Criteria Decision Aid, UTility Additive theory.**

I. Introduction

UNMANNED Aerial Systems (UAS) have been employed in a diverse range of military applications to date. With respect to civilian applications, geographically sparse countries, such as Australia, have considerable potential for utilization of UAS in asset management, search and rescue, remote sensing operations and atmospheric observation [1]. However, seamless operation of UAS platforms within the National Airspace System (NAS) is required to ultimately realize this potential [2].

From a regulatory perspective, demonstrating an Equivalent Level Of Safety (ELOS) to that of a human piloted aircraft will be one of the requirements for the integration of Unmanned Aircraft (UA) into the NAS [3]. Most literature indicate that this capability can be realized through the inclusion of intelligent control architectures [4], [5].

Intelligent control architectures [5] are hierarchical methodologies which allow for the automation of aspects of UAS operations which would otherwise require a human in the loop. This research component focuses on the automation of the trajectory planning aspect of intelligent control systems. Trajectory planning is the generation of feasible collision free flight tracks. In the presence of communications failures, the inclusion of automated trajectory planning processes can allow for the UAS to safely continue autonomous operations even at lower altitudes where terrain must be treated as a hazard.

Automating the trajectory planning process is however, non-trivial and some challenges include: incorporation of complex platform dynamics, trajectory optimization to meet mission objectives, and the guarantee that the generated solution is collision free. Additionally, during typical manned and unmanned operations, multiple mission objectives may exist. These objectives can include platform safety (collision avoidance and consideration of platform constraints); successful completion of the mission; minimizing fuel, time, and/or distance; or minimizing deviation from the current flight track. These mission objectives are discussed in further detail in Section III.

The application of Multi-Criteria Decision Aid (MCDA) techniques [6] can potentially allow for convergence to a solution which better reflects overall mission requirements. Alternatively, continuous missions where UA are used in a coordinated fashion (e.g. to provide sensor coverage for mobile ground nodes) are not considered here, as sensor modeling is outside the scope of this research.

Even with greater levels of autonomy present onboard, due to the potential risks of platform failure, UAS operations are expected to be continuously monitored by Human Decision Makers (HDMs) at the ground station. Franke [7] states that with increasing levels of autonomy onboard, UAS operators move away from direct control of the platform towards a management by exception control paradigm. Management by exception occurs when the UAS performs planning and execution and informs the HDM of its current and future actions. The operator has the option to veto or override the current plans and revert to a lower control paradigm if required.

It is important to note, that during the decision making process, the HDM will apply the operator's own values, priorities and preferences for a given decision problem [8]. Different human operators may possess varying viewpoints on whether a given solution is acceptable or to be vetoed. The analysis of expert decision data gathered from a set of human operators may provide a deeper understanding of objectives considered and the preferences they apply during the decision making process. Incorporating this information into a multi-criteria optimization process can potentially allow automated trajectory planners to better encapsulate mission criteria considered by supervising HDMs [7].

This paper presents a new method for the encapsulation

P. Narayan is a PhD Candidate, Queensland University of Technology, Australia.

P. Meyer is an Associate Professor, Institut Télécom, Télécom Bretagne, UMR CNRS 3192 Lab-STICC, France.

D. Campbell is an Associate Professor, Queensland University of Technology, Australia.

Manuscript received Aug 1, 2011; revised Apr 2, 2012.

of the preferences of a human pilot, through multi-criteria trajectory planning for autonomous UAS. An outline of automated trajectory planning approaches and related work is given in Section II. Section II also outlines the candidate trajectory generation process, where the solution is generated through the concatenation of primitives through the application of Manoeuvre Automaton (MA) theory. Section III provides an overview of the Multi-Criteria Decision Aid (MCDA) process in context with the research problem. Section IV then presents the application of the MCDA process to the current research problem to formulate preferences from HDM decision data. Simulation results presented in section V, demonstrate how the inclusion of the human expert decision data can allow for the generation of feasible trajectories which encapsulate aspects of the candidate decision maker's preferences. Finally, conclusions are presented in Section VI.

II. Autonomous trajectory planning overview

The implementation of an automated trajectory planning system onboard UAS platforms has the benefit of overcoming potential ground station link issues. This allows for continued autonomous UAS operations in cluttered environments, even in the presence of communications link failures. However, automating the trajectory planning process is non-trivial and some challenges include: incorporation of complex platform dynamics and trajectory optimization to meet given mission requirements.

The inclusion of vehicle dynamics during the trajectory planning process, allows for the generation of flight trajectories which take platform constraints into account. Vehicle dynamics are used to calculate the performance envelope representing a set of bounds on the UA during flight, which if exceeded, can result in platform instability.

A. Flight trajectory representation

Flight trajectories can be represented through a variety of methods, including, spline based or geometric approximations. Polynomial or spline based techniques [9], [10] place control points in a particular order to generate the desired trajectory. Geometric based techniques require the concatenation of aircraft flight manoeuvres to form a smooth flight track [11], [12], [13], [14].

The actuator control power available on fixed wing platforms is finite; this leads to a transient period where the vehicle does not remain in a state of equilibrium while the platform transitions between different states of trim. While the platform remains in a state outside equilibrium (trim conditions), attitude rates will be non-zero. During periods when the platform is not in a state of equilibrium, the trajectory planner must account for platform attitude rates as a component of the overall aircraft performance envelope. A candidate method which allows for the inclusion of attitude rates as a component of overall performance bounds is Manoeuvre Automaton (MA) theory [15], [16].

B. Manoeuvre automaton theory

MA theory, proposed by Frazzoli et. al. [15], [16] is an approach for the efficient solution of motion planning problems for time-invariant non-linear, dynamical control systems with symmetries, such as UA's. MA is a hybrid representation of the dynamics of a vehicle, consisting of a finite collection of two types of motion primitives: trims and manoeuvres. Trim primitives represent the vehicle during a state of equilibrium whilst manoeuvre primitives characterize the vehicle operating outside a state of equilibrium. At each point in time the vehicle is either in a trim condition or performing a manoeuvre between two trim conditions [17].

The following section provides a brief overview of trim and manoeuvre primitive representation for fixed wing UA. For a detailed overview of MA theory and primitive representation, refer to [16], [17].

1) Trim primitive representation: The hybrid representation consists of a continuous UA state $s(t)$ or (**s**), where **s** = ([position], [attitude], [attitude rate], speed) = $([x(t), y(t), z(t)], [\phi(t), \theta(t), \psi(t)], [\dot{\phi}(t), \dot{\theta}(t), \dot{\psi}(t)], u_0)$ and predefined q (e.g. coordinated turn). The initial platform state $s(t_i)$ = $\mathbf{s}_i$ reaches a final state $s(t_f)$ = $\mathbf{s}_f$ due to the execution of a given q and corresponding jump time τ_q (where $\tau_q \in [0, t_f - t_i]$); this can be represented as [17]:

$$\begin{aligned} \mathbf{s}_f &= \mathbf{s}_i + \tau_q \dot{\mathbf{s}}_q \\ t_f &= t_i + \tau_q \end{aligned} \tag{1}$$

where $\dot{\mathbf{s}}_q$ is the time rate of change of the aircraft's continuous state variables (e.g. due to the execution of a coordinated turn primitive).

Using MA theory, trim primitives for fixed wing platforms can be generated by placing the body fixed roll $(\dot{\phi})$ and pitch $(\dot{\theta})$ rates to zero and maintaining a constant speed (u_0), roll (ϕ) and pitch (θ) angle for the duration (τ) of the primitive execution.

Trim primitives were generated in simulation within the MATrix LABoratory (MATLAB) programming environment using a six Degree of Freedom (DOF) flight dynamics model based on the Aerosonde Unmanned Aircraft (UA) dataset (available in the Aerosim blockset). Six predefined trim primitives have been implemented in simulation including: cruise, coordinated turn, climb, descent, helical climb and helical descent. Let $\mathbf{q} = \{q_1, q_2, ..., q_n\}$ represent the set of trim primitives.

2) Manoeuvre primitive representation: During the execution of a manoeuvre primitive, the UAS does not have to remain in a state of equilibrium. For a fixed wing platform, the body fixed attitude rate constraint applied is $(\dot{\phi}, \dot{\theta})$ = $(\dot{\phi}_{max}, \dot{\theta}_{max})$. In this paper, manoeuvre primitives are employed to connect two trim primitives, if required (i.e. $(\phi, \theta)_i$ $\neq$ $(\phi, \theta)_q$) (Figure 1).

C. Generating feasible trajectories through concatenation

A smooth, nominal, feasible and collision free trajectory is required for safe guidance of the UA from its current state to the desired goal state. The final trajectory is formed

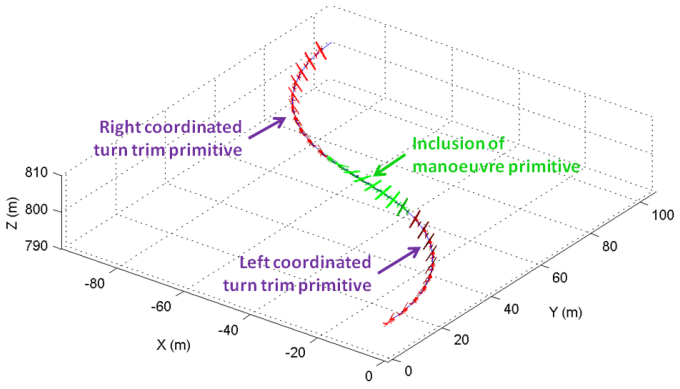

Fig. 1. Visual representation of trim primitive concatenation with inclusion of attitude rate constraints through inclusion of manoeuvre primitive

through sequential concatenation of selected trim primitives and corresponding manoeuvre primitives, if required, where each trim primitive selected for execution can be considered as a stage. For example, Figure 1 presents the concatenation of left and right coordinated turn trim primitives, where the inclusion of a manoeuvre primitive allows for consideration of platform attitude rate constraints. Concatenation without optimization, may lead to the generation of trajectories which do not accurately represent mission objectives, thus a decision strategy is required to generate trajectories which best meet one or more mission criteria.

Dynamic programming (DP) [18] has been previously employed in related research [15], [17], [19] for the optimization of feasible trajectories generated through the application of MA theory. DP is a sequential optimization method which finds the least cost (optimal) solution from a set of alternative solutions. To guarantee that the optimal solution is found, the DP algorithm must consider all possible alternatives across all stages.

In comparison to the application of DP to trajectory planning with respect to a generic graph search implementation, the current UA position can be treated as the current node. Each possible state the platform can reach through the execution of currently stored trim primitives must be treated as neighboring nodes. Expanding each neighboring node would cause the algorithm to grow exponentially in computational complexity for each additional stage considered in the overall optimization process [20].

To decrease the computational complexity and resulting time to plan, Frazzoli et. al [15], [16] apply a hybrid architecture to the motion planning problem for rotary aircraft. The hybrid architecture involves integration of DP (optimized over single stage) with other optimization algorithms such as Rapidly exploring Random Trees (RRT) [15] and Model Predictive Control (MPC) [17].

The research presented in this paper uses the DP search algorithm but limits the search to single stage optimization. This converts the DP algorithm to a greedy search implementation, which essentially chooses the trim primitive, trim execution time and manoeuvre execution time with the least cost for the each stage in a sequential manner. The UAS position after execution of the optimal trim primitive is taken as the next node for expansion, and continues until the goal is reached.

Executing a DP search algorithm iteratively over a single stage without explicit consideration for future stages ensures that the computational complexity and resulting time to plan remain comparatively small. However, not considering all stages during the optimization process means that global trajectory solution optimality and completeness cannot be guaranteed.

Global path solution optimality and completeness can be guaranteed through the application of an intelligent control architecture with a mission/path planning layer which uses a deterministic search algorithm to generate an optimal set of waypoints from the current position to the goal [20]. In addition, during operations in dynamic and partially known environments, a greedy motion planning implementation must suffice as it most likely, will not be possible to find a global trajectory solution due to limited environment representation.

D. Summary of findings

This section presented the generation of feasible trajectories for fixed wing platforms using MA theory. Planning in 3D environments was possible through the formulation of common aircraft flight manoeuvres. Attitude rate constraints were included through the inclusion of manoeuvre primitives to allow for increased trackeability.

Single stage DP optimization was selected for the generation of trajectories in a computationally efficient manner. However, it was found that research applying MA theory [15], [17], [19], [21] did not consider HDM's decision preferences during DP optimization.

As trust has an influence on the operator's reliance on automation [22], operating at higher autonomy levels [23] will require the HDM to have a sense of confidence that the automated onboard systems are making correct decisions [24]. During the decision making process, the HDM will apply the operator's own values, priorities and preferences for a given decision problem [8]. Furthermore, different human operators may possess varying viewpoints on whether a given solution is acceptable or should be vetoed.

The following section investigates application of MCDA methodologies to represent HDM and mission requirements more accurately during the generation of feasible trajectories based on MA theory.

III. MCDA STRATEGY

Many problems can be solved through the application of decision analysis and decision aid techniques. The decision aid process guides the HDM with finding the most appropriate solution from a given set of alternatives. Each alternative will have one or more characteristics (criteria) which represent different dimensions in which an HDM can view the desirability of a given alternative by.

During the course of flight operations, the pilot/UAS operator may have to consider multiple criteria in order to achieve mission success. Examples of mission criteria generally include: achieving the mission goal/s; safety of the

vehicle, the environment and the public at all times; mission efficiency (minimizing time, fuel, and/or cost); and/or limiting operations to below or above a specified altitude ceiling. Mission objectives and their priorities can dynamically change at any point during UAS operations (at the discretion of the mission commander).

Decision making during autonomous trajectory planning requires the selection of the most suitable feasible collision free trajectory with respect to one or more criteria. Gigerenzer et al. [25] have shown that HDMs do consider multiple criteria during real-life decision making processes. Therefore, the use of MCDA methodologies during autonomous trajectory planning may allow for convergence to a solution which better reflects overall mission requirements. The following section presents an overview of MCDA techniques.

A. MCDA overview

MCDA is a category of decision aid methods in which decisions are formulated through the comparison of alternatives with respect to multiple criteria. Many MCDA techniques [26] have been published to date which can be used to determine the most suitable alternative, or to sort or rank a set of alternatives. MCDA techniques can roughly be divided into two categories: on the one hand additive Multiple Attribute Value Theory (MAVT) [27], [28], which aims at aggregating the multiple points of view into a unique synthesis criterion, and, on the other hand outranking methods [29] which aim at comparing the decision alternatives pairwisely and accept incomparability.

MCDA allows for the encapsulation of the HDM's decision style through the inclusion of preference information and a relevant set of criteria. Preference information can take various forms, among which, for example, is the relative importance of each criterion to the HDM. The capture of these human preferences is called preference elicitation and depends on the HDM's individual decision experiences and training that they may have received. The following section presents a generic overview of the MCDA process and its use in the context of automated flight operations.

B. MCDA process

The MCDA process requires the implementation of algorithms which attempt to mimic aspects of the HDM's decision making style and take into account their preferences. Classically, an MCDA process can be divided into the following four steps [30]:

1) *Determining the relevant criteria and alternatives;*
2) *Evaluating the alternatives on all the criteria;*
3) *Eliciting the HDM's preferences related to the current decision problem;*
4) *Combining the evaluations and the preferential information to solve the decision problem and produce a decision recommendation.*

In the sequel we detail each of these steps in our context.

1) Determining relevant criteria and alternatives: The DP algorithm is applied to this research for optimal trajectory selection, but the search is limited to single stage only. Optimization using DP search over one stage involves selection of the optimal trim primitive (q) and corresponding jump time or primitive duration (τ_q) from a predefined set of trim primitives $(\mathbf{q})$ and possible jump times $(\boldsymbol{\tau}_q)$ for each stage in an iterative manner. Let $\boldsymbol{\tau}_q = \{\tau_{q,1}, \tau_{q,2}, ..., \tau_{q,i}\} \in [0, t_f - t_i]$ represent the discrete possible set of possible jump times for each q.

Each discrete τ_q, for a given q, can be represented as a unique decision alternative, as it will result in a different final state if executed. Let A be the set of such alternatives (a visual representation of an example A is presented in Figure 4). A is dependent on the number of q within the automaton and the number of discrete τ_q samples (i_q) representing each q. Thus, the total number of alternatives for (m) trim primitives is:

$$\text{Total Alternatives} = \sum_{n=1}^{m} i(q_n) \quad \forall q_n \in \mathbf{q} \tag{2}$$

The criteria represent different dimensions with which an alternative can be viewed by. In literature, it was found that Frazzoli et. al [15] applied two such criteria: minimizing euclidean distance between current UA state $(\mathbf{s}_p)$ position (x_p, y_p, z_p) or $(\mathbf{p})$, and goal state $(\mathbf{s}_g)$ position (x_g, y_g, z_g) or $(\mathbf{g})$ (criterion $\text{crit}_{||\mathbf{g}-\mathbf{p}||}$); and minimizing platform yaw (ψ_p) and goal yaw (ψ_g) angles (criterion $\text{crit}_{|\Delta\psi|}$) during optimal manoeuvre selection.

If $\text{crit}_{||\mathbf{g}-\mathbf{p}||}$ and $\text{crit}_{|\Delta\psi|}$ do not completely encapsulate the HDM's decision strategies, then the inclusion of additional criteria allows the onboard trajectory planner to take into account certain aspects of the mission which cannot be considered using only the current two criteria. In the presence of external disturbances, execution of turns with higher bank angles (even if within performance bounds) places the platform at higher risk of instability [31]. One aspect of platform safety can be implicitly considered through the inclusion of criterion $\text{crit}_{|\phi|}$ which focuses on the minimization of high platform roll angles (ϕ_p).

The second additional (criterion $\text{crit}_{|z_g - z_p|}$) considers the minimization of the altitude of the goal (z_g) and current state (z_p). For decision scenarios where the goal is not at the same altitude as the platform, this criterion captures how focused a HDM is on reaching the required altitude.

2) Evaluating alternatives on all the criteria: In order to perform decisions on the set of alternatives (e.g. generating the most appropriate decision or ranking/sorting with respect to the HDM's preferences), an evaluation scale needs to be attached to each of the criteria. Each alternative is then evaluated by placing a cost to go (from current state to the alternate state) on all attached criteria.

Whilst Frazzoli has not explicitly defined the criteria applied in literature [15], $\text{crit}_{||\mathbf{g}-\mathbf{p}||}$ can be expressed in 3D planning space as the euclidean distance between the goal (g) and the current position (p). A lower cost $(c_{||\mathbf{g}-\mathbf{p}||})$ is placed on q which drive the UAS platform closer to the goal (3).

$\text{crit}_{|\Delta\psi|}$ allows for greater control of the heading of the platform. For this research (ψ_g) represents the direction to

next goal. The cost ($c_{|\Delta\psi|}$) can be calculated by taking the absolute difference between the desired (ψ_d) and absolute platform headings (ψ_a). Alternatives with a resulting ψ_a closer to ψ_d will have a lower cost placed on them (4).

$$c_{||\mathbf{g}-\mathbf{p}||} = ||\mathbf{g}-\mathbf{p}|| \in [\min_{\mathbf{q}} ||\mathbf{g}-\mathbf{p}_q||, \max_{\mathbf{q}} ||\mathbf{g}-\mathbf{p}_q||] \quad (3)$$

$$c_{|\Delta\psi|} = |\psi_d - \psi_a| \in [0, \pi] \quad (4)$$

The evaluation of $\text{crit}_{|\phi|}$ has been performed by placing a greater cost ($c_{|\phi|}$) on trim primitives which are executed with higher roll angles (5). Finally, a lower cost ($c_{|z_g-z_p|}$) is placed on trim primitives which decrease the relative vertical distance between the platform altitude (z_p) and goal altitude (z_g) for $\text{crit}_{|z_g-z_p|}$ (6).

$$c_{|\phi|} = |\phi| \in [0, \phi_{max}] \quad (5)$$

$$c_{|z_g-z_p|} = |z_g - z_p| \in [\min_{\mathbf{q}} |z_g - z_{p_q}|, \max_{\mathbf{q}} |z_g - z_{p_q}|] \quad (6)$$

Each candidate HDM may have their own perception of the relative importance of each criteria and thus the desirability of the alternatives presented. If an automated onboard trajectory planner applies multiple criteria without accounting for the relative importance placed on each criteria by the candidate HDM, the trajectory solution maybe quite different from what the UAS operator expects. The following section provides an overview of methods present in literature which formulate preferences through the analysis of HDM decision data.

3) Eliciting the HDM's preferences related to the current decision problem: This elicitation can be performed either by questioning the HDM directly on the values of the various preferential parameters, or by extracting this information via a disaggregation technique from an order on some alternatives which the HDM is able to express.

To capture such expert knowledge in a direct way, one can use the MACBETH technique (Measuring Attractiveness by a Categorical Based Evaluation Technique) [32]. MACBETH's goal is to build a cardinal scale measuring the attractiveness of options through a learning process involving an interactive software. The HDM is asked to perform qualitative pairwise comparisons regarding his preferences between various evaluation levels and express himself on a scale reaching from *very weak* to *extreme*.

A well-known disaggregation approach is UTA (UTilité Additive) [33]. Here the HDM is tasked first with ranking a few well-known alternatives. Linear Programming (LP) techniques are then used to perform an ordinal linear regression in order to determine a preference model which is consistent with the HDM's overall preferences. Both MACBETH and UTA approaches generate value functions and weighting vectors which correspond to the HDM's preferences. These can then be used in additive MAVT based decision algorithms. UTA has been selected as the candidate method for the conversion of HDM decision strategies to preference parameters as it allows for more intuitive capture if the alternatives are presented to the HDM visually through a Graphical User Interface (GUI) (Figure 5).

Let A be the set of alternatives and $J = \{h_1, \ldots, h_n\}$ be the set of n criteria where $h_1 = \text{crit}_{||\mathbf{g}-\mathbf{p}||}$ etc.. Each criterion can be seen as a real-valued function on the set A. Let $h(a)$ be the vector of evaluations of alternative a of A on the criteria of J. The criteria aggregation model in UTA is assumed to be an additive value function of the following form:

$$\nu(h(a)) = \sum_{i=1}^{n} w_i \nu_i(h_i(a)) \quad \forall a \in A \quad (7)$$

where $\nu_i(h_i(a))$ $(i = 1, \ldots, n)$ are real-valued functions called marginal value functions which are normalized between 0 and 1, w_i is the weight of criterion i, and $\nu(h(a))$ is the overall value function. A higher value of $\nu_i(h_i(a))$ is associated with a better alternative on criterion i.

In UTA, the ranking given by the HDM on a subset of alternatives is transformed into a set of linear constraints on ν, which are added to the UTA disaggregation LP (see [33] for further details). The objective of this LP is to minimize the gap between the initial ranking given by the HDM and the one produced by the aggregation model. The output of the UTA LP is a set of value functions and associated weights which represent the HDM's preferences, based on the input ranking that they have provided.

4) Determining a ranking of the alternatives: In order to determine which alternative is the most attractive for the HDM, a ranking of all the alternatives is computed. This allows the HDM direct access not only to the "best" solution, but to the remaining solutions and corresponding rankings.

The aggregation technique used here is based on additive MAVT and requires the value functions and the weights obtained by the UTA technique. Consequently, the aggregation formula (7) is applied on the set of feasible alternatives. Thus, each of the alternatives gets an overall value, to rank them from the most attractive to the least attractive one.

C. Summary of findings

This section presented a brief overview of MCDA and outlines the MCDA process to generate feasible trajectories which applied aspects of candidate HDMs decision styles. Alternatives were defined as unique feasible sampled states which could be reached by the UAS platform. Criteria represented different dimensions with which a HDM could view the desirability of each alternative by.

The UTA disaggregation technique was selected to formulate preference information to represent HDM preferences and priorities for each criteria. An additive MAVT decision strategy would then be applied to incorporate HDM preferences during the aggregation of value functions representing mission criteria.

The following section details the application of the proposed MCDA process to the current research problem to generate trajectory solutions which more accurately represent HDM and mission objectives.

IV. Application of the Proposed MCDA Process to the Current Research Problem

This section applies the MCDA process to the current research problem to formulate preferences which represent HDM's mission priorities. The following section details the HDM data capture process.

A. Expert knowledge capture and decision modeling strategies

One way of viewing the trajectory planning problem using single stage optimization is that the candidate HDM is presented with unique decision scenarios, where the HDM must select the most appropriate trajectory segment in an iterative manner until the mission is completed. During trajectory selection, HDMs' preferences may vary depending on the decision scenario presented to them, for example, individual HDM may have a different set of preferences in mind when the UA is closer to the goal as opposed to decision scenarios where the UA position is farther from the goal.

1) Decision Scenarios: A decision scenario can be defined as the relative difference between the goal and UA position $(x_g - x_p, y_g - y_p, z_g - z_p)$ or $(x_{g-p}, y_{g-p}, z_{g-p})$, and the relative orientation of the UA with respect to the desired direction at the goal (ψ_d). The goal (next waypoint) is represented as a spherical region with radius R_g to ensure that a tolerance is provided for more practical waypoint capture during online planning (Figure 2).

The inclusion of attitude rate constraints through manoeuvre primitives results in unique A for a given ϕ_p; the effect of attitude rates is more pronounced on A of shorter duration (τ_q) (Figure 4). Thus, each unique decision scenario can be represented as $(x_{g-p}, y_{g-p}, z_{g-p}, \psi_d, \phi_p)$. Figure 2 shows an example decision scenario presented to the candidate HDM.

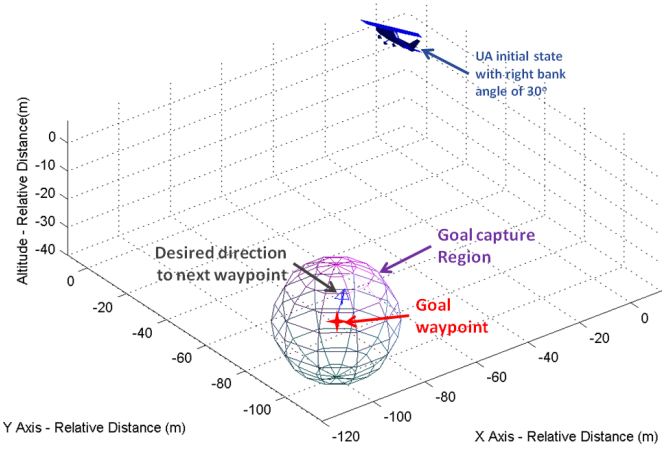

Fig. 2. Example decision scenario presented to HDM

The capture of HDM decision data for each unique decision scenario only provides a discrete snapshot of the candidate HDM's decision preferences. To perfectly model a HDM's decision style, would require the HDM completing an extremely large (approaching infinity) set of unique decision scenarios; this is not feasible. Thus, a sampled set of unique scenarios (which represent a discrete approximated subset of unique decision scenarios) are presented to the HDM via the GUI during data capture.

The decision scenario set is pseudo-randomly selected; this enables consistency during decision analysis, as different HDM's are presented with the same decision sets during data capture. Furthermore, increasing the number of decision scenarios in the sampled set also increases the overall decision scenario resolution.

One hundred and twenty unique decision scenarios are completed by each HDM to form a bank of decisions. The decision scenario set is separated into five subsets of 24 decision scenarios; this allows HDMs to complete the decision scenario set over several sessions (Table I). Each subset captures the HDM's preferences when the UA requires climbing, maintaining altitude or descending to reach the goal position. At each altitude level (z_{g-p}), 2D goal location (x_{g-p}, y_{g-p}), and ψ_d are pseudorandomly generated to capture the HDM's preferences for different goal states. Figure 3 presents an overlay of all decisions scenarios presented to the HDM in subset 1.

TABLE I
Decision Scenario Set Separated into Five Subsets

Subset	ϕ_p Radians	$(\max(x_{g-p}), \max(y_{g-p}))$ (metres, metres)	(z_{g-p}) metres	ψ_d Radians
1	$-\pi/3$	(100,100)	(-20,0,20)	$[0{:}\pi/4{:}2\pi]$
2	$\pi/3$	(100,100)	(-20,0,20)	$[0{:}\pi/4{:}2\pi]$
3	0	(100,100)	(-20,0,20)	$[0{:}\pi/4{:}2\pi]$
4	0	(400,400)	(-80,0,80)	$[0{:}\pi/4{:}2\pi]$
5	0	(1000,1000)	(-200,0,200)	$[0{:}\pi/4{:}2\pi]$

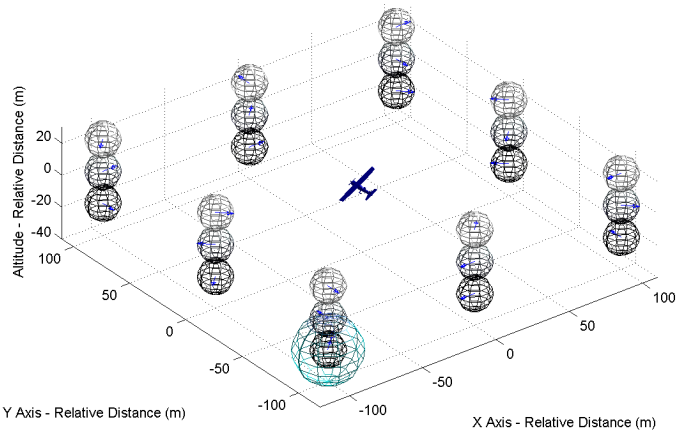

Fig. 3. Overlay of decision scenarios presented to HDM in decision subset 1

2) Alternatives: Alternatives represent unique current platform states $(\mathbf{s}_p)$ which can be reached by the UA from the initial state $(\mathbf{s}_i)$ through the execution of a predefined q and corresponding τ_q, whilst taking into account UA dynamic constraints. Applying MA theory, A is generated through the discretization of trim primitives $(\mathbf{q})$ (representing common fixed wing aircraft flight manoeuvres) and executed over a set of possible jump times $(\boldsymbol{\tau}_q)$. The trim primitives include straight and level flight, climb, descend, coordinated turn, helical ascent and helical descent manoeuvres.

The Federal Aviation Administration (FAA) [34] lists the typical maximum value of platform wingload factor as 3.8. This research applies a more conservative arbitrary value of 2.2 resulting in a maximum bank angle (ϕ_{max}) of approximately 61° and a minimum stall speed (V_{stall}) of 29 m/s during coordinated turns; all trim primitives are executed at a constant velocity of 30 m/s. The maximum angle of climb (γ_{max}) for the aerosonde flight model at 30 m/s is approximately 7.5°.

The alternative set (A) consists of 516 unique states (during data capture), generated through the discretization of platform dynamics. Flight manoeuvres are discretized by applying a sampling resolution to ϕ_p and γ_p of 10° and 7.5° respectively; this results in 39 trim primitives manoeuvres (Figure 4). Setting maximum duration (τ_{max}) of primitives to allow the platform to perform a complete coordinated turn provides the HDM with a broader range of alternatives to select from, but also results in longer trim primitives if ϕ_p is low. Additionally, τ_q is adjusted proportionally to $||\mathbf{g}-\mathbf{p}||$ to ensure that alternatives scale with the euclidean distance between waypoints. Finally, a variable primitive sampling rate assures that the distance between alternatives along each primitive is less than the diameter of the region of tolerance encompassing the goal.

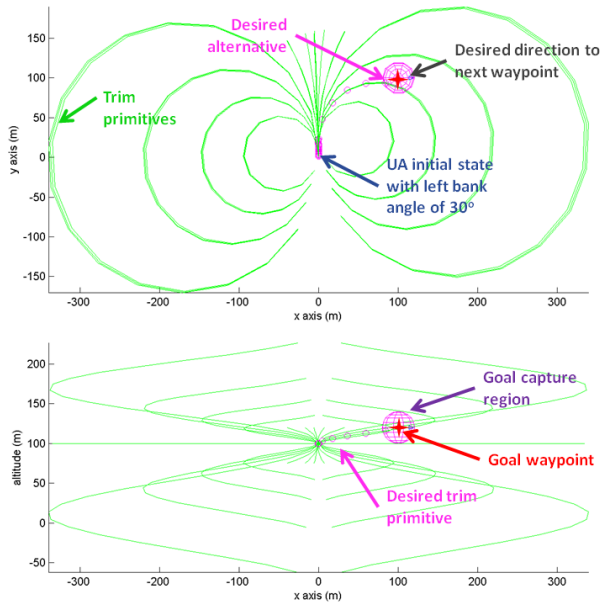

Fig. 4. Alternatives generated for decision scenario 1 (Table II)

Each HDM is sequentially presented with decision scenarios and tasked with selecting what they consider to be the most suitable trim primitive to execute for each particular scenario. Whilst research has been conducted into the development of Human Machine Interfaces (HMIs) and Heads Up Displays (HUDs) to improve the supervision and control of UAS [35], [36], [37], no relevant research regarding data capture of HDM decisions for trajectory planning was found. In order to elicit human expert decision preferences, a GUI was developed to generate a set of simulated decision scenarios, and to capture the corresponding candidate HDM's decision patterns. The following section provides an overview of the GUI's development and functionality.

3) Graphical User Interface: The GUI was developed using MATLAB's GUI Design Environment (GUIDE). This GUI did not explicitly apply UA HMI development methodologies, rather it was iteratively improved through HDM feedback during functionality testing.

Figure 5 presents the GUI, where components are represented in a different colours, to further highlight their position on the GUI. The screen component presents the HDM with the current decision scenario and automaton. Desired primitive selection is performed using the select policy button, where the HDM cycles through trim primitives using navigational buttons and adjusts the primitive length using a slider function. Additional information is also available to the user including; UA state information, primitive type, and absolute and relative (to goal) position information. Climb, constant altitude and descent primitives are also presented in different colours to provide greater clarity when the HDM transitions between decision scenarios of different altitudes.

The HDM decisions are then used to form preferences, for inclusion into an additive MAVT based Automated Decision System (ADS), that generates trajectories which incorporate aspects of HDM decision strategies. The following section provides an overview of the formulation of preferences through the application of UTA theory to the current research problem.

B. Preference formulation using UTA

UTA is applied to all decision sets completed by the HDM to form a selectable bank of preference data. The following sections present three experiments on three different problem formulations. A least cost formulation (LC-2) represents the inclusion of $\text{crit}_{||\mathbf{g}-\mathbf{p}||}$ and $\text{crit}_{|\Delta\psi|}$ with equal preference weighting as the reference solution. UTA-2 represents the inclusion of $\text{crit}_{||\mathbf{g}-\mathbf{p}||}$ and $\text{crit}_{|\Delta\psi|}$ where UTA is applied to generate value functions and weighting values using the candidate HDM's decision data. UTA-4 describes the inclusion of all four criteria presented in Section III-B1 where value functions and weighting values are again generated from candidate HDM decision data using UTA.

1) LC-2: An ADS applying the LC-2 decision algorithm generates trajectories where $\text{crit}_{||\mathbf{g}-\mathbf{p}||}$ and $\text{crit}_{|\Delta\psi|}$ are given equal preference. The costs $c_{||\mathbf{g}-\mathbf{p}||}$ and $c_{|\Delta\psi|}$ can be equivalently represented as value functions $\nu(||\mathbf{g}-\mathbf{p}||)$ and $\nu(|\Delta\psi|)$ respectively (8)(9).

$$\nu(||\mathbf{g}-\mathbf{p}||) = 1 - \left(\frac{c_{||\mathbf{g}-\mathbf{p}||}}{\max_{\mathbf{q}}\left(c_{||\mathbf{g}-\mathbf{p}||}\right)}\right) \tag{8}$$

$$\nu(|\Delta\psi|) = 1 - \left(\frac{c_{|\Delta\psi|}}{\pi}\right) \tag{9}$$

LC-2 may not accurately represent mission requirements as the candidate HDM may have their own perceptions on which criteria's are relevant to the current mission scenario and the preference given to each relevant criteria.

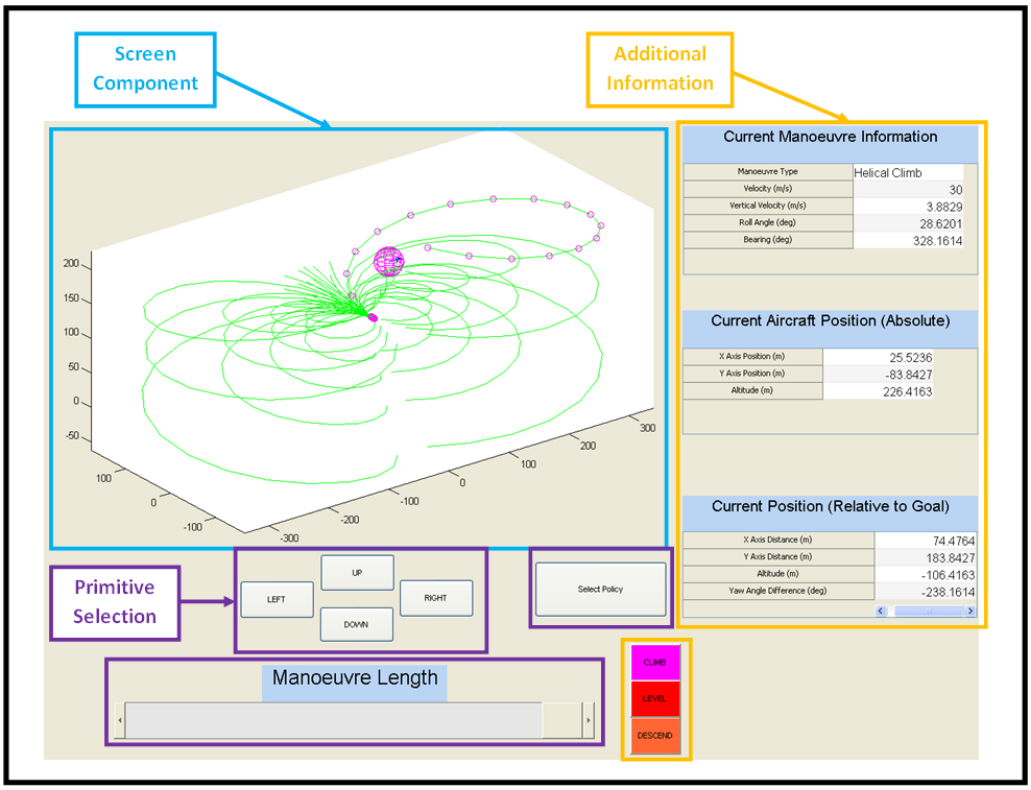

Fig. 5. Graphical User Interface developed for HDM data capture

2) UTA-2: UTA theory is applied to the HDM decision sets to generate value functions and weighting values for $\text{crit}_{||\mathbf{g}-\mathbf{p}||}$ and $\text{crit}_{|\Delta\psi|}$ which provide a mathematical representation of the HDM's decision style for each given scenario. Figure 6 shows the value functions generated using UTA theory for the sample decision scenario (Figure 2) when $\text{crit}_{||\mathbf{g}-\mathbf{p}||}$ and $\text{crit}_{|\Delta\psi|}$ are applied. Note that the weighting value is embedded within each value function (the maximum value of the value function corresponds to the weight coefficient of Formula 7).

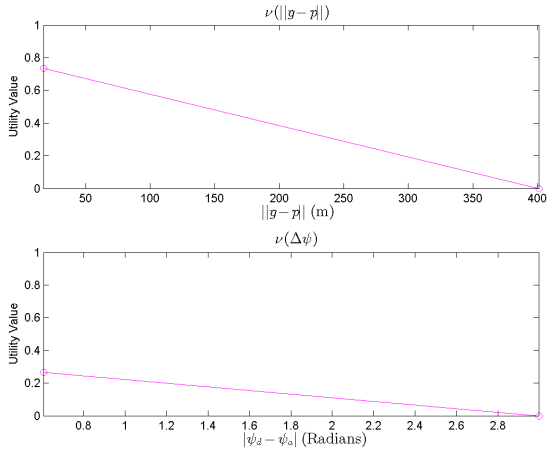

Fig. 6. UTA value functions (UTA-2 with HDM 2 dataset) representing HDM preferences for sample decision scenario (Figure 2)

3) UTA-4: In order to investigate if the inclusion of additional criteria can allow UTA to represent HDM decisions with further accuracy, UTA-4 applies two additional criteria ($\text{crit}_{|\phi|}$ and $\text{crit}_{|z_g-z_p|}$) during preference formulation using UTA theory. Figure 7 shows the value functions generated using UTA theory for the sample decision scenario (Figure 2) when the two previous and two additional criteria are applied.

The following section compares UTA-4 and UTA-2 against LC-2 (reference least cost solution) to investigate the HDM decision modeling accuracy of UTA theory using HDM datasets captured.

C. Accuracy of UTA

This section presents the results of the statistical analysis performed to quantify the accuracy of UTA in modeling HDM decisions. The ADS completes the same decision scenarios as the HDM using UTA-4, UTA-2 and LC-2 algorithms. The primitive types, number (m) and samples per primitive (i) applied during ADS decision making are listed in Table II. The alternative set (3900 alternatives) is sampled at a higher resolution than during data capture (516 alternatives) to reduce the possibility of aliasing during collision detection.

The decision sets computed by the ADS are compared against the HDM decisions in pairwise fashion to determine the mean (μ) relative difference between HDM and ADS decisions, with respect to four comparisons. The notation used in this section to represent the μ of the relative difference between HDM and ADS decisions, with respect to four comparisons is presented in Table III.

If the mean of the relative difference between the HDM and ADS decisions (for the comparisons) is zero, then the

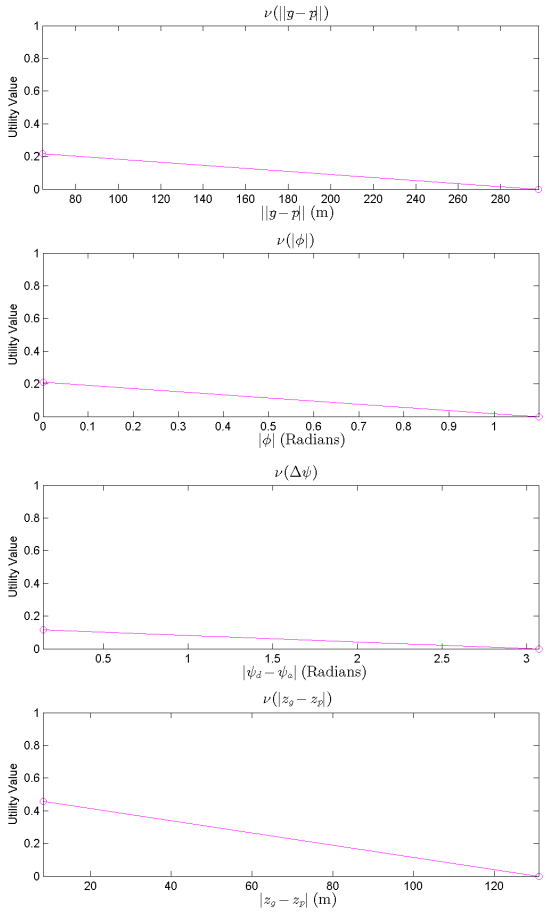

Fig. 7. UTA value functions (UTA-4 with HDM 2 dataset) representing HDM preferences for sample decision scenario (Figure 2)

TABLE II
PRIMITIVE TYPE, NUMBER AND SAMPLES PER PRIMITIVE APPLIED DURING ONLINE SIMULATIONS

Primitive Type	**Primitive No.** (m)	**Primitive Samples** (i)
Straight and Level	1	100
Coordinated Turn	12	100
Constant Climb	1	100
Helical Climb	12	100
Constant Descend	1	100
Helical Descend	12	100

ADS is generating decisions which are the same or similar to the HDM, for the given decision scenario set [38]. Thus, the null hypothesis (H_0) for this statistical analysis can be stated as, the mean difference between HDM and ADS decision values (for each comparison) are equal (i.e.. $H_0 : \Delta\mu = \mu_{(HDM)-(UTA-4)} = \mu_{(HDM)-(UTA-2)} = \mu_{(HDM)-(LC-2)} = 0$).

TABLE III
NOTATION USED IN THE REPRESENTATION OF μ RELATIVE DIFFERENCE BETWEEN HDM AND ADS DECISIONS

Comparison between HDM and ADS positions	**Notation (long)**	**Notation (short)**
μ euclidean distance	$\mu(\|\|\mathbf{p}_{(HDM)} - \mathbf{p}_{(ADS)}\|\|)$	$\mu(\Delta\mathbf{p})$
μ ψ	$\mu(\|\psi_{(HDM)} - \psi_{(ADS)}\|)$	$\mu(\Delta\|\psi\|)$
μ ϕ	$\mu(\|\phi_{(HDM)} - \phi_{(ADS)}\|)$	$\mu(\Delta\phi)$
μ relative altitude	$\mu(\|z_{(HDM)} - z_{(ADS)}\|)$	$\mu(\Delta z)$

Figure 8 presents the mean value for each comparison, computed for all decision scenarios. The application of UTA-2 generated decisions which had lower $\mu(\Delta\mathbf{p})$, $\mu(\Delta\psi)$, $\mu(\Delta\psi)$, and $\mu(\Delta z)$ in comparison to the automated generation of decisions using LC-2 . This implies that $\text{crit}_{||\mathbf{g}-\mathbf{p}||}$ and $\text{crit}_{|\Delta\psi|}$ are relevant and considered by the HDM during the decision making process. Additionally, the inclusion of additional criteria (UTA-4) resulted in comparisons having lower means than UTA-2. As $\mu_{(HDM)-(UTA-4)} < \mu_{(HDM)-(UTA-2)}$ (for almost all comparisons), the following sections will focus on comparing the relative means of $\mu_{(HDM)-(UTA-4)}$ and $\mu_{(HDM)-(LC-2)}$ to determine if UTA-4 accurately models aspects of the HDM decision preferences.

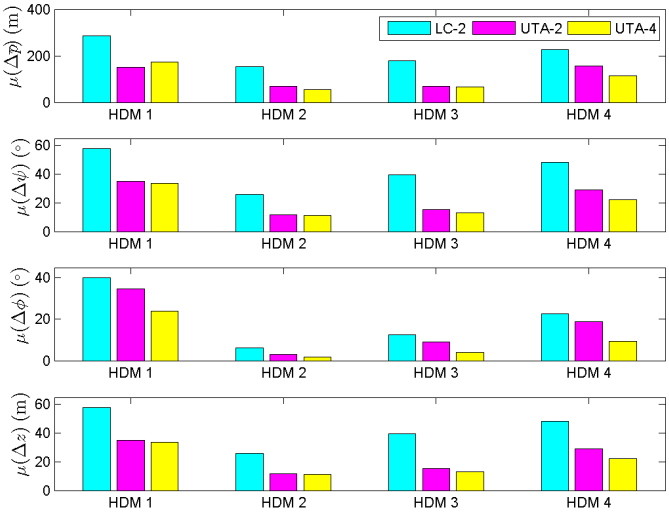

Fig. 8. Average error comparison between human and automated trajectory decisions for all decision sets

Whilst $\mu_{(HDM)-(UTA-4)} < \mu_{(HDM)-(LC-2)}$ for all comparisons, it cannot be stated with confidence that the ADS with UTA-4 closely models HDM decisions for the given decision scenario set. One statistical test to compare multiple means and determine if the means are not significantly different is ANalysis Of VAriance (ANOVA). However, an ANOVA test is limited in that it can only confirm if one of the comparative means is significantly different, but not which one [39]. Tukey's Honestly Significant Difference (HSD) test is one post-hoc analysis which can be applied to the ANOVA results, to determine which means are significantly different from the reference mean (μ_{HDM}).

A One-way ANOVA with Tukey's HSD post-hoc analysis is performed to determine if a significant difference exists between the reference mean (μ_{HDM}), and the means of UTA-4 (μ_{UTA-4}) and LC-2 (μ_{LC-2}) decisions (for each comparison). Tukey's HSD test applies Confidence Limits (CL's) on each difference of mean $(\Delta\mu)$ where the CL is the product of the Studentized Range Statistic (Q) and Standard Error (SE) (10).

$$\Delta\mu \pm CL = \mu_{HDM} - \mu_{ADS} \pm (Q \times SE) \qquad (10)$$

SE is calculated by dividing the Mean Standard Deviation (MSD) from the ANOVA results by the square root of the number of decision scenarios ($N = 120$) attempted by each HDM. The critical value of Q is calculated to be 4.12 using the studentized range statistic table with the following parameters (Number of means ($K = 3$), Degrees of Freedom ($DF = (K \times N) - N = 357$), and rate of Type I error ($\alpha = 0.01$) A lower value of α results in a more conservative (larger Q value) bounds for a smaller risk of Type I error (incorrect rejection of H_0). Table IV presents the application of Tukey's HSD formula to determine which means (for each comparison) are significantly different from μ_{HDM}.

The results of Tukey's HSD test (Table IV) indicate that there is not a significant difference between means for Δp, $\Delta\phi$, and Δz comparisons for HDM 2 and 3, and the corresponding UTA-4 decision sets. Thus, UTA-4 closely matches aspects of HDM 2 and 3's decisions preferences for the given decision scenario set. Further analysis of the individual HDM 2 and 3's offline decision set shows how the UAS platform is expected to perform during autonomous operations with the inclusion of HDM preferences.

1) HDM 2 offline decisions: Figure 9 presents a box plot comparing the absolute median platform ϕ values for HDM 2, ADS UTA-4 and ADS LC-2 decisions. HDM 2 generally executed flight manoeuvres where $\phi \in [20°, 40°]$ (Figure 9). The ADS with the inclusion of HDM preferences (UTA-4) executed primitives within a similar range to HDM 2. The LC-2 formulation does not explicitly take ϕ limitations into account, subsequently the ADS using an LC-2 optimization had greater variance in the roll angle range of the primitives executed (Figure 9).

Based on the results of Tukey's HSD test, it is expected that UTA-4 using HDM 2's decision data will not periodically execute manoeuvres with higher roll angle values unlike the ADS using an LC-2 optimization (Figure 10). This is desired as the execution of flight manoeuvres with higher wing loading values has a greater possibility of platform instability [31].

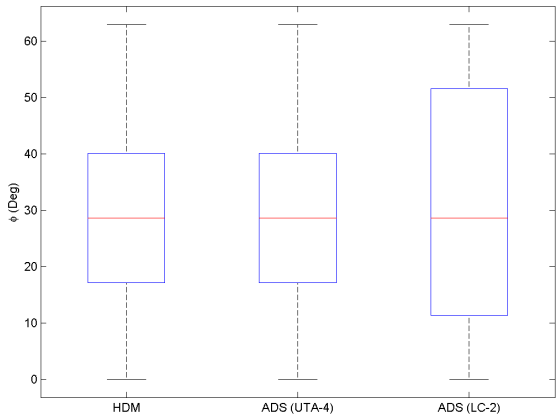

Fig. 9. Box plots comparing UAS platform ϕ for offline trajectories selected by HDM 2, ADS LC-2 and ADS UTA-4 decisions

2) HDM 3 offline decisions: Figure 11 presents a box plot comparing the median $|z_g - z_p|$ values for HDM 3, ADS UTA-4 and ADS LC-2 decisions. All data points greater than one and half times the inter quartile range from each respective median were classified as outliers.

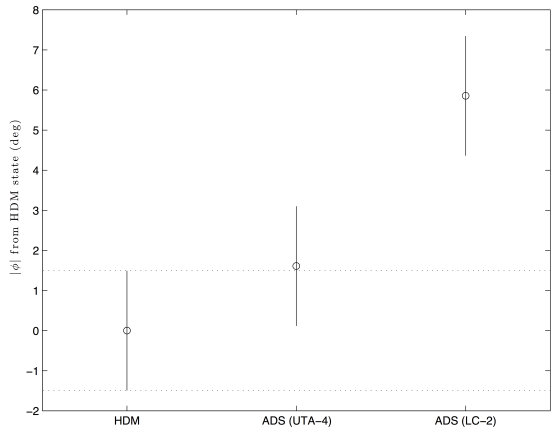

Fig. 10. Tukey's HSD test results for $|\phi_{(HDM)} - \phi_{(ADS)}|$ comparison between HDM 2, UTA-4 and LC-2 decisions

HDM 3 selected flight manoeuvres where a greater preference was placed on minimizing the altitude of the platform z_p with respect to the goal altitude z_g. Since LC-2 only considers altitude minimization as a component of $\text{crit}_{||\mathbf{g}-\mathbf{p}||}$, it was found that LC-2 optimization had greater variance during offline simulation in comparison to the HDM and UTA-4 trajectory solutions (Figure 11).

Based on the results of Tukey's HSD test, it is expected that UTA-4 with the inclusion of HDM 3's decision data is more likely to generate trajectories with lower $|z_g - z_p|$ values in comparison to the ADS using an LC-2 optimization (Figure 12). This reflects on the candidate HDM's preference on maintaining a similar altitude to the goal which can be beneficial for certain missions e.g. airborne surveillance or video capture.

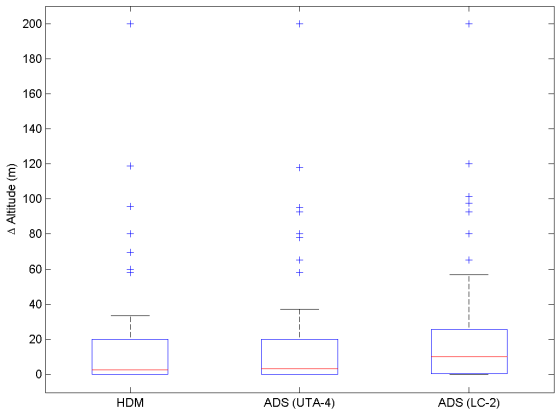

Fig. 11. Box plots comparing UAS platform $|z_g - z_p|$ for offline trajectories selected by HDM 3, ADS LC-2 and ADS UTA-4 decisions

D. Summary of findings

This section presented the application of the MCDA process to the current research problem. The expert knowledge capture process was outlined where the HDM uses a GUI to select the

TABLE IV
$\Delta\mu$ FOR ALL COMPARISONS AND HDMS USING TUKEY'S HSD FORMULA

HDM	Comparison Against ADS	$\|\|p_{(HDM)} - p_{(ADS)}\|\|$ $\Delta(mean)$ $\pm CL$	Significant Difference	$\|\psi_{(HDM)} - \psi_{(ADS)}\|$ $\Delta(mean)$ $\pm CL$	Significant Difference	$\|\phi_{(HDM)} - \phi_{(ADS)}\|$ $\Delta(mean)$ $\pm CL$	Significant Difference	$\|z_{(HDM)} - z_{(ADS)}\|$ $\Delta\mu$ $\pm CL$	Significant Difference
1	UTA4	173.6 ± 97.75	Yes	33.44 ± 13.21	Yes	23.80 ± 9.66	Yes	15.29 ± 8.82	Yes
	LC2	280.6 ± 97.75	Yes	58.53 ± 13.21	Yes	39.54 ± 9.66	Yes	22.65 ± 8.82	Yes
2	UTA4	55.27 ± 60.90	No	11.08 ± 7.28	Yes	1.61 ± 2.99	No	14.27 ± 14.51	No
	LC2	136.9 ± 60.90	Yes	23.70 ± 7.28	Yes	5.85 ± 2.99	Yes	22.77 ± 14.51	Yes
3	UTA4	66.86 ± 76.59	No	12.90 ± 9.64	Yes	4.02 ± 5.62	No	6.65 ± 8.17	No
	LC2	183.4 ± 76.59	Yes	39.63 ± 9.64	Yes	12.51 ± 5.62	Yes	13.72 ± 8.17	Yes
4	UTA4	113.2 ± 76.10	Yes	22.17 ± 9.72	Yes	9.48 ± 6.48	Yes	12.74 ± 8.68	Yes
	LC2	219.7 ± 76.10	Yes	48.51 ± 9.72	Yes	22.29 ± 6.48	Yes	26.10 ± 8.68	Yes

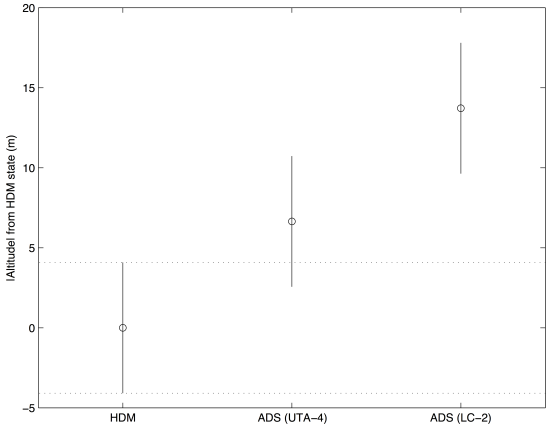

Fig. 12. Tukey's HSD test results for $|z_{(HDM)} - z_{(ADS)}|$ comparison between HDM 2, UTA-4 and LC-2 decisions

most desirable alternative from a set of alternatives for each unique decision scenario presented. UTA theory was applied to form HDM preferences from the decision data captured. The HDM preferences were applied to the ADS to automate the generation of trajectory decisions which encapsulated aspects of the candidate HDM's preferences. A One-way ANOVA with Tukey's HSD post-hoc analysis was applied to determine how closely the ADS with UTA-4 encapsulates aspects of the HDM's decision preferences.

It was found that the ADS with the inclusion of HDM preferences, generated decisions which were closer to the HDM decisions captured using the GUI implementation (Figure 8). Furthermore, the results of Tukey's HDS test showed that the difference betweens $\mu_{(HDM)-(UTA-4)}$ for HDM 2 and 3 is not significantly different for $\mu(\Delta\mathbf{p})$, $\mu(\Delta\psi)$, and $\mu(\Delta z)$ comparisons. Potential reasons for UTA-4 not closely matching decisions of HDM 1 and 4 include; additional criteria considered by HDMs 1 and 4 which are not defined in this research and the representation of HDM preferences as linear functions only.

The following section demonstrates the inclusion of HDM preferences to generate trajectories which encapsulate aspects of the candidate HDMs decision preferences, in low altitude flights through simulated 3D environments.

V. RESULTS

This section presents the automated generation of feasible trajectories through the concatenation of primitives using MA theory (Section II-B). The automated process mimics aspects of the HDM decision process through the inclusion of preferences formulated using UTA theory from HDM expert data captured.

A. Simulation setup

A 3D terrain environment (Figure 13) was setup in MATLAB to simulate mission scenarios where the UAS assignment includes, safe and efficient navigation through a set of globally optimal mission waypoints [40]. The simulation has been performed on a computer with an Intel Core 2 quad core processor operating at 2.8 GHz to simulate how the inclusion of human expert data to the motion planning problem can lead to the generation of UAS flight trajectories which encapsulates aspects of the HDM decision process.

The ADS is tasked with generating an optimized, feasible and collision free trajectory through all mission level waypoints until the goal is reached (Figure 13). The waypoints can either be selected by the user, or provided by an automated mission planner. We use a near globally optimal multi-criteria mission planning solution by Wu [40] for the low altitude trajectory planning results in simulated environments.

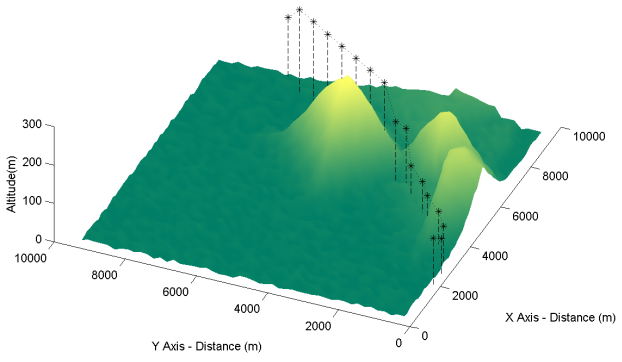

Fig. 13. Simulated mission environment with waypoints (terrain simulation 1)

The ADS generates a set of alternatives for each stage by selecting the number of primitives (m) and the samples per primitive (i) (Section III-B1). A large set of alternatives provides a greater number of final states which the platform can

reach and a higher resolution of the region within the platforms performance bounds. Consequently, a large set of alternatives requires a greater computational effort and subsequently a longer time to plan. Table II lists the primitive types, (m) and (i) applied during online trajectory planning.

B. Preference selection during online planning

During online trajectory planning, the automated decision algorithm compares the current online decision scenario to the set of decision scenarios presented to the candidate HDM offline (Figure 3). A least squares formulation (13) is applied to map the HDM preference data for the offline decision scenario which most closely matches the current online decision scenario.

The least squares formulation minimizes the normalised difference between the current online $(x_{g-p}, y_{g-p}, z_{g-p}, \psi_d, \phi_p)_{ON}$ and all offline decision scenario sets $(\mathbf{x_{g-p}}, \mathbf{y_{g-p}}, \mathbf{z_{g-p}}, \boldsymbol{\psi_d}, \boldsymbol{\phi_p})_{\mathbf{OFF}}$. Let the normalised terms be defined as $(\hat{\mathbf{x}}, \hat{\mathbf{y}}, \hat{\mathbf{z}}, \hat{\boldsymbol{\psi}}, \hat{\boldsymbol{\phi}})$ and the set of offline decision scenarios be defined as $\mathbf{OFF} = \{OFF_1, OFF_2, ..., OFF_N\}$. Terms $\hat{\mathbf{x}}, \hat{\mathbf{y}}, \hat{\mathbf{z}}$ can be normalised in the following manner. For example, in the case of $\hat{\mathbf{x}}$ where N Offline decision scenarios are available and $i \in \{1, ..., N\}$:

$$\hat{x}_i = \frac{\left|x_{(g-p)_{ON}} - x_{(g-p,i)_{OFF}}\right|}{\max_{\mathbf{OFF}}\left(\left|x_{(g-p)_{ON}} - \mathbf{x_{(g-p)_{OFF}}}\right|\right)} \tag{11}$$

The terms $\hat{\boldsymbol{\psi}}$ and $\hat{\boldsymbol{\phi}}$ can be normalised in the following manner:

$$\hat{\phi}_i = \frac{\text{mod}_{\ 2\pi}\left|\phi_{p_{ON}} - \phi_{p,i_{OFF}}\right|}{\max_{\mathbf{OFF}}\left(\ \text{mod}_{\ 2\pi}\left|\phi_{p_{ON}} - \boldsymbol{\phi}_{\mathbf{p_{OFF}}}\right|\right)} \tag{12}$$

$\hat{\boldsymbol{\psi}}$ is not included in the least squares formulation as it adds bias during long range mission planning where distance between waypoints is the same as, or exceeds $\max_{\mathbf{OFF}}\left(||\mathbf{x_{g-p}}, \mathbf{y_{g-p}}, \mathbf{z_{g-p}}||\right)_{\mathbf{OFF}}$. The least squares formulation for N offline scenarios where $i \in \{1, ..., N\}$ is:

$$LSQR_i = \min_i\left(\sqrt{(\hat{x})_i^{\ 2} + (\hat{y})_i^{\ 2} + (\hat{z})_i^{\ 2} + (\hat{\phi})_i^{\ 2}}\right) \tag{13}$$

Preferences are extracted from the HDM offline decision scenario with the lowest least squares formulation value $(LSQR_i)$. The ADS then selects q and corresponding τ_q values by applying the selected HDM preferences (represented as weighted value functions) to the weighted sum formulation (7). The execution of q and with a corresponding τ_q allows for the calculation of the next platform state $(\mathbf{s_f})$. This process occurs iteratively until a trajectory computed reaches $\mathbf{s_g}$; the location of current waypoint (W_k). After reaching the current waypoint (designated as the local goal), the ADS updates $\mathbf{s_g}$ where $\mathbf{s_g} = W_{k+1}$. The ADS performs this process in an iterative manner until the UA has traversed across all waypoints sequentially and reaches the destination.

The following section presents the results of the online simulations where the automated trajectory mimics aspects of HDM decision styles through the inclusion of preferences formulated using HDM decision data via UTA theory.

C. Simulation results

For the inclusion of collision avoidance during 3D trajectory planning using MA theory, the terrain map data is used to cull trim primitives which are below a specified terrain height, at the given grid location (Figure 14). This ensures that an optimized collision free trim primitive can be selected for each stage from the remaining collision free set of primitives. Each stage represents a new trim primitive segment, where the concatenation of all stages forms the overall trajectory generated by the ADS.

The automated LC-2 solution is used as a reference and compared to the solution generated by the ADS with the inclusion of the candidate HDM's decision patterns through UTA theory. The comparative trajectory applies the candidate HDM's decision style through the inclusion of HDM preferences formulated using UTA-4.

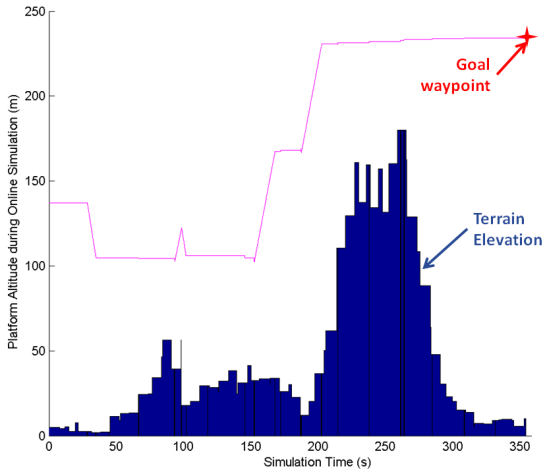

Fig. 14. UAS platform altitude during simulation (UTA-4 with HDM 3 dataset) (terrain simulation 1)

1) Terrain Simulation 1: HDM 3's dataset was applied to UTA-4 and compared to the reference solution generated by LC-2 (Figure 15). Analysis of HDM 3's offline dataset showed that the HDM placed a greater preference on minimizing $\text{crit}_{|z_g - z_p|}$ (Figure 11). Subsequently, during online trajectory planning in simulated environments, UTA-4 generated collision free trajectories which had lower $|z_g - z_p|$ on average than LC-2 (Figure 16).

2) Terrain Simulation 2: HDM 2's dataset was applied to UTA-4 and compared to the reference solution generated by LC-2 (Figure 17). HDM 2 preferred to minimize platform ϕ variance during the offline simulation set (Figure 9). LC-2 has a higher preference for $\text{crit}_{|\Delta\psi|}$ which leads to the selection of manoeuvres which exhibit a low $c_{|\Delta\psi|}$ (4). This can result in the selection of primitives on the edge of the platforms wing loading performance bounds as LC-2 does not explicitly consider $\text{crit}_{|\Delta\phi|}$ during optimization. This can be viewed in Figure 18 where LC-2 exhibits higher maximum ϕ values than UTA-4.

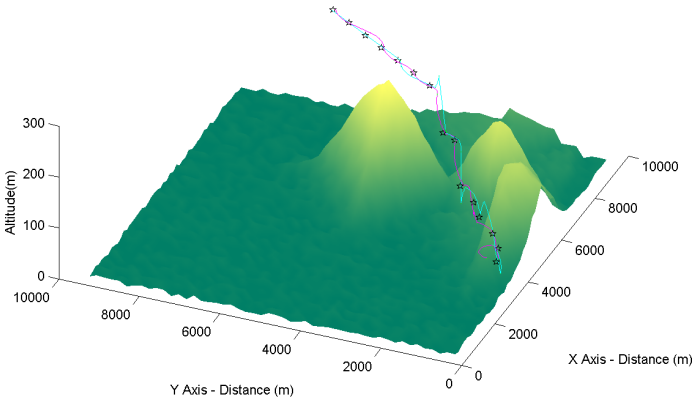

Fig. 15. Comparing trajectories from LC-2 solution and UTA-4 with HDM 3 dataset (terrain simulation 1)

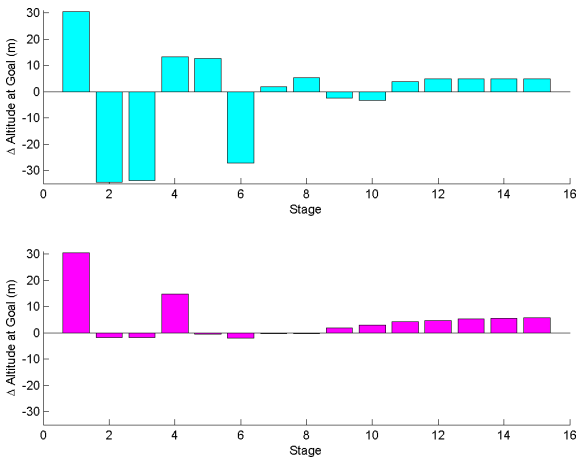

Fig. 16. Comparing UAS platform ΔAltitude at goal for LC-2 solution and UTA-4 with HDM 3 dataset (terrain simulation 1)

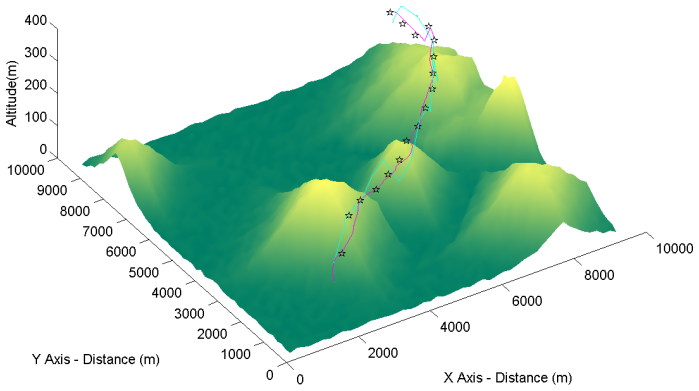

Fig. 17. Comparing Trajectories from LC-2 solution and UTA-4 with HDM 2 Dataset (terrain simulation 2)

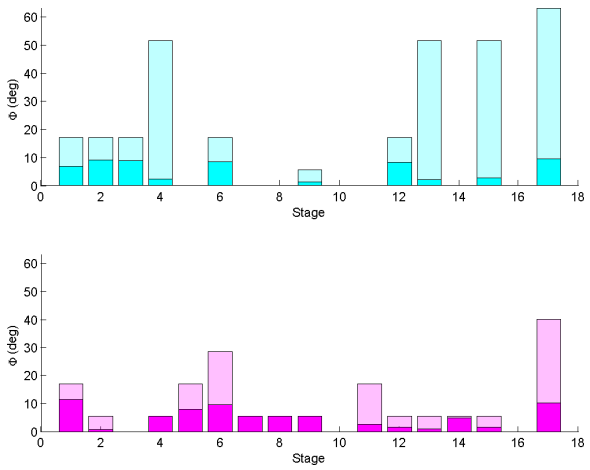

Fig. 18. Comparing UAS Platform Mean and Maximum ϕ (per stage) for LC-2 solution and UTA-4 with HDM 2 Dataset (terrain simulation 2)

VI. Discussion and Conclusions

This paper presented a new approach for the inclusion of human expert cognition into an autonomous trajectory-planning algorithm for Unmanned Aerial Systems (UAS). Collision detection methods were applied to ensure feasible safe trajectories could be generated in low altitude environments with terrain present. Expert decision data was gathered using a Graphical User Interface (GUI), allowing for the quantification of the human decision making process. Aspects of human cognition were applied to MA theory to generate feasible 3D collision free trajectories which were optimized to generate similar decisions with respect to the candidate HDM during autonomous operations.

It has been demonstrated that HDM decision preferences can be better represented in automated trajectory planning systems through the inclusion of HDM decision data through the application of UTA MCDA techniques. It is expected that better encapsulation of HDM decision styles may increase the HDM's sense of trust with onboard automated planning systems, and subsequently, increase the acceptance of the autonomous trajectory solution. Future work could be conducted to quantify the increase in acceptance of the automated trajectory solution by the candidate HDM. One method for quantifying acceptance could be measuring how often a HDM vetos the automated trajectory solutions presented to them.

Using automated decision algorithms which apply human expert decision preferences may also result in increase confidence in UAS operations over populated regions and potentially bring civilian UAVs closer to being operated autonomously in the NAS.

Acknowledgment

The authors would like to thank and acknowledge the support of the Australian Research Centre for Aerospace Automation (ARCAA), the Queensland University of Technology (QUT) and Télécom Bretagne throughout this research project. The authors would also like thank and acknowledge Paul Wu for providing terrain data and the corresponding set of optimized mission waypoints.

References

[1] S. Wegener, "Uav autonomous operations for airborne science missions," American Institute of Aeronautics and Astronautics, Tech. Rep., 2004.

[2] EUROCONTROL, "Specifications for the use of military unmanned aerial vehicles as operational air traffic outside segregated airspace," Tech. Rep., 25 April 2006.

[3] M. T. DeGarmo, "Issues concerning integration of unmanned aerial vehicles in civil airspace," MITRE, Center for Advanced Aviation System Development, Tech. Rep., 2004.

[4] J. Boskovic, R. Prasanth, and R. Mehra, "A multilayer control architecture for unmanned aerial vehicles," in *Proceedings of the American Control Conference*, U. o. Cincinnati, Ed., vol. 3, 2002, pp. 1825–1830.

[5] R. P. Bonasso, D. Kortenkamp, D. P. Miller, and M. G. Slack, "Experiences with an architecture for intelligent, reactive agents," in *International Joint Conference on Artificial Intelligence*, 1995.

[6] P. Vincke, *Multicriteria Decision-Aid*. Wiley UK, 1992.

[7] J. Franke, V. Zaychik, T. Spura, and E. Alves, "Inverting the operator/vehicle ratio: Approaches to next generation uav command and control," in *Unmanned Systems North America*, 2005.

[8] P. Meyer, "Progressive methods in multiple criteria decision analysis," Ph.D. dissertation, 2007.

[9] I. K. Nikolos, K. P. Valavanis, N. C. Tsourveloudis, and A. N. Kostaras, "Evolutionary algorithm based offline/online path planner for uav navigation," *IEEE Transactions on Systems Man and Cybernetics Part B-Cybernetics*, vol. 33, no. 6, pp. 898–912, 2003.

[10] K. B. Judd and T. W. McLain, "Spline based path planning for unmanned air vehicles," in *AIAA Guidance, Navigation, and Control Conference and Exhibit*, vol. AIAA-2001-4238, 2001.

[11] E. Anderson, R. Beard, and T. McLain, "Real-time dynamic trajectory smoothing for unmanned air vehicles," *IEEE Transactions on Control Systems Technology*, vol. 13, no. 3, pp. 471–477, 2005.

[12] E. Gagnon, C. Rabbath, and M. Lauzon, "Heading and position receding horizon control for trajectory generation," in *The Proceedings of the American Control Conference*, 2005, pp. 134–139.

[13] Y. Kuwata, "Real-time trajectory design for unmanned aerial vehicles using receding horizon control," Master of Science, 2003.

[14] D. Rathbun, S. Kragelund, A. Pongpunwattana, and B. Capozzi, "An evolution based path planning algorithm for autonomous motion of a uav through uncertain environments," in *21st Digital Avionics Systems Conference*. IEEE, 2002.

[15] E. Frazzoli, M. Dahleh, and E. Feron, "A hybrid control architecture for aggressive maneuvering of autonomous helicopters," in *Proceedings of the 38th IEEE Conference on Decision and Control*, vol. 3, 1999, pp. 2471–2476.

[16] ——, "Maneuver-based motion planning for nonlinear systems with symmetries," *IEEE Transactions on Robotics and Automation*, vol. 21, no. 6, pp. 1077–1091, 2005.

[17] T. Schouwenaars, B. Mettler, E. Feron, and J. How, "Robust motion planning using a maneuver automaton with built-in uncertainties," in *AIAA Aerospace Sciences and Exhibit*, 2003.

[18] R. Bellman, "On the theory of dynamic programming." *National Academy of Sciences*, vol. 38, p. 716, 1952.

[19] L. Singh, J. Plump, M. McConley, and B. Appleby, "Software enabled control: Autonomous agile guidance and control for a uav in partially unknown urban terrain," in *AIAA Guidance, Navigation, and Control Conference and Exhibit*, 2003.

[20] S. M. LaValle, *Planning Algorithms*. New York: Cambridge University Press, 2006.

[21] N. D. Richards, M. Sharma, and D. G. Ward, "A hybrid a*/automaton approach to on-line path planning with obstacle avoidance," in *AIAA 1st Intelligent Systems Technical Conference*, vol. 1, 2004, pp. 141–157.

[22] J. D. Lee and K. A. See, "Trust in automation: Designing for appropriate reliance," *HUMAN FACTORS*, vol. 46, no. 1, pp. 50–80, 2004.

[23] R. Parasuraman, T. Sheridan, and C. Wickens, "A model for types and levels of human interaction with automation," *IEEE Transactions on Systems, Man, and Cybernetics - Part A: Systems and Humans*, vol. 30, no. 3, 2000.

[24] M. L. Cummings, S. Bruni, S. Mercier, and P. J. Mitchell, "Automation architecture for single operator, multiple uav command and control," *The international Command and Control Journal*, vol. 1, pp. 1–24, 2007.

[25] G. Gigerenzer, P. Todd, and A. R. Group, "Simple heuristics that make us smart," Tech. Rep., 1999.

[26] J. Figueira, S. Greco, and M. Ehrgott, *Multi Criteria Decision Analysis: State of the Art Surveys*. Boston: Springer, 2005.

[27] P. C. Fishburn, *Utility Theory for Decision Making*. New York: John Wiley and Sons, Inc., 1970.

[28] R. Keeney and H. Raiffa, *Decision with multiple objectives: Preferences and value tradeoffs*. Cambridge University Press, 1976.

[29] B. Roy, "Classement et choix en prsence de points de vue multiples (la mthode electre)," *la Revue d'Informatique et de Recherche Oprationelle (RIRO)*, vol. 8, pp. 57–75, 1968.

[30] E. Triantaphyllou, B. Shu, S. N. Sanchez, and T. Ray, "Multi-criteria decision making: An operations research approach," *Encyclopedia of Electrical and Electronics Engineering*, vol. 15, pp. 175–186, 1998.

[31] F. A. Administration, *Performance Maneuvers*, 2nd ed. Aviation Supplies and Academics, Inc., 2004, ch. 9.

[32] C. Bana e Costa and J. Vansnick, "A theoretical framework for measuring attractiveness by a categorical based evaluation technique (macbeth)," in *XIth Int. Conf. on MultiCriteria Decision Making*, 1994, p. 1524.

[33] E. Jacquet-Lagreze and J. Siskos, "Assessing a set of additive utility functions for multicriteria decision-making, the uta method," *European Journal of Operational Research*, vol. 10, pp. 151–164, 1982.

[34] "Airworthiness standards: Normal, utility, acrobatic, and commuter category airplanes," 1996.

[35] I. Ashdown, H. Blackford, N. Colford, and F. Else, "Common hmi for uxvs: Design philosophy and design concept," BAE Systems, Tech. Rep., 2010.

[36] F. De Crescenzio, G. Miranda, F. Persiani, and T. Bombardi, "A first implementation of an advanced 3d interface to control and supervise uav (uninhabited aerial vehicles) missions," *Presence: Teleoperators and Virtual Environments*, vol. 18, no. 3, 2009.

[37] B. J. A. van Marwijk, C. Borst, M. Mulder, M. Mulder, and M. M. van Paassen, "Supporting 4d trajectory revisions on the flight deck: Design of a humanmachine interface," *The International Journal of Aviation Psychology*, vol. 21, no. 1, pp. 35–61, 2011.

[38] D. C. Hoaglin, F. Mosteller, and J. W. Tukey, *Fundamentals of Exploratory Analysis of Variance*. John Wiley & Sons, 1991.

[39] A. Rubin, *Statistics for Evidence-Based Practice and Evaluation*. Wadsworth Publishing Co. Inc., 2009.

[40] P. P. Wu, D. A. Campbell, and T. Merz, "On-board multi-objective mission planning for unmanned aerial vehicles," in *IEEE Aerospace Conference*, 2009.

Pritesh Narayan completed his bachelor's degree in Aerospace Avionics Engineering with first class honors at QUT in 2005. Pritesh is currently a PhD candidate at ARCAA QUT (Brisbane, Australia). His research investigates the inclusion of human expert cognition into autonomous trajectory planning, for UAS operating in environments with real time constraints present.

Patrick Meyer is currently an Associate Professor at Télécom Bretagne (France) and a member of the Lab-STICC laboratory of the French National Center for Scientific Research. Patrick obtained his PhD in Mathematics and Engineering Science, jointly from the Univ. of Luxembourg and the Engineering Faculty of Mons (Belgium) in 2007. He has also worked four years as a researcher at the Univ. of Liége (Belgium) and four years as a teaching and research assistant at the Univ. of Luxembourg.

Duncan Campbell is an Associate Professor in the School of Engineering Systems at QUT and is also the Acting Director of ARCAA. Duncan is currently the President of Australasian Association for Engineering Education (AAEE) and previously served as IEEE Queensland Chair for the joint chapters of Control Systems, and Robotics and Automation (2008-2009). He also leads an international group on the internationalisation of the engineering curriculum.